Spin-dependent electron momentum density in Fe_3Si and Fe_3Al

2000 J. Phys.: Condens. Matter 12 7229

(http://iopscience.iop.org/0953-8984/12/32/307)

J. Phys.: Condens. Matter **12** (2000) 7229–7241. Printed in the UK PII: S0953-8984(00)13603-3

Spin-dependent electron momentum density in Fe_3Si and Fe_3Al

E Żukowski†, A Andrejczuk†, L Dobrzyński†‡, S Kaprzyk§, M J Cooper‖, J A Duffy‖ and D N Timms¶

† Institute of Experimental Physics, University of Bialystok, ul. Lipowa 41, 15-424 Bialystok, Poland
‡ Laboratoire de Mineralogie et Cristallographie, Université Pierre et Marie Curie (Paris VI), 4, place Jussieu, 75252 Paris, France
and
The Soltan Institute for Nuclear Studies, 05-400 Otwock-Swierk, Poland
§ Academy of Mining and Metallurgy, Al. Mickiewicza 30, 31-214 Kraków, Poland
‖ Department of Physics, University of Warwick, Coventry CV4 7AL, UK
¶ Division of Physics, University of Portsmouth, Portsmouth P01 2DZ, UK

E-mail: csmc@spec.warwick.ac.uk

Received 28 April 2000

Abstract. Circularly polarized synchrotron radiation of energy 200 keV has been used to study the spin dependent electron momentum distributions in Fe_3Al and Fe_3Si single crystals at room temperature through magnetic Compton profile measurements. The experiments were carried out for the crystallographic directions [100], [110] and [111] in Fe_3Si, and [100] and [111] in Fe_3Al. These results show that there is a more significant negative conduction electron spin polarization in both alloys than neutron data indicate and it is similar to that in pure iron. The overall characteristics of the experimental magnetic Compton profiles, as well as directional anisotropies, were found to be qualitatively similar for both compounds; however the anisotropy is higher in the case of Fe_3Si. The majority and minority spin band profiles have been extracted and show that large anisotropies are associated with the latter. Their calculated anisotropy at low momenta was fully confirmed. The *ab initio* KKR calculation reproduces the Fe_3Si profiles relatively well, but a 'fixed-spin moment approach' was needed in order to describe the Fe_3Al spin density momentum distribution.

1. Introduction

1.1. The alloy structure and properties

The Fe_3Al and Fe_3Si alloys have the DO_3 crystallographic structure which, in turn, is related to the $L2_1$ structure typical of Heusler alloys. It can be viewed as constructed from four interpenetrating fcc sublattices shifted by one-quarter of the body diagonal with respect to each other. Four atoms occupy the positions A (0,0,0), B (1/4, 1/4, 1/4), C (1/2, 1/2, 1/2) and D (3/4, 3/4, 3/4) in the unit cell. In ideally ordered systems A, B and C sites are occupied by Fe and Si and Al atoms are present at the D site only. The structure in Fe_3Si is stable and the degree of order is known to be very high (previous studies of Fe_3Si have assumed complete order [1]); however Fe_3Al is easily subject to disorder, which is dependent on sample history. For example, the degree of the long-range order of the Fe_3Al sample studied [2] was equal to 90% (±2%).

0953-8984/00/327229+13$30.00

Both alloys are ferromagnetic: the Curie temperatures and lattice constants are 780 K and 830 K, 0.579 nm and 0.566 nm for Fe_3Al and Fe_3Si, respectively [3]. The corresponding saturation magnetization moments measured at room temperature with a vibrating sample magnetometer yielded values of 4.80(5) μ_B and 4.90(5) μ_B per formula unit for Fe_3Si and Fe_3Al respectively. The former is close to the value of 4.95(5) μ_B deduced from a recent study of $(Fe/V)_3Al$ alloys [4]. Both moments are consistent with the values of 4.79 μ_B (Fe_3Si) and 4.97 μ_B (Fe_3Al) reported in [5], as well as the earlier data in [1] and [2]. The Fe atoms carry two distinctly different values of magnetic moment. For example moments of 1.5 μ_B on Fe at the A, C sites and 2.2 μ_B at the B sites are published in [2] for Fe_3Al, while values of 1.07 μ_B at A, C sites and 2.23 μ_B at B sites for Fe in Fe_3Si are given in [1].

DO_3-type alloys of composition X_3Z have been the subject of a number of papers [1, 2, 5–9]. In particular the different environments of Fe at B and A, C sites make it possible to study the influence of the neighbourhood on the magnetic moments. Because the lattice parameters of Fe_3Si and Fe_3Al are 2% different, the influence of the atomic volume can also be studied. Electronic structures for Fe_3Si and for Fe_3Al are published in [10] and [11] respectively. They show that the basic magnetic properties of the two materials (site magnetic moments, Curie temperatures) are similar. However, neutron scattering by spin waves [12] shows that the main exchange interactions are almost three times smaller in Fe_3Al than in Fe_3Si, which may be attributed to the changed Fe–Fe separation. The mechanical properties of both alloys are also dissimilar and the location of transition metal atoms substituting for iron also differs (see [13] and references therein). These observations indicate a strong coupling of magnetic and lattice degrees of freedom in these alloys. This difference between the two alloys must originate in the electronic structure and should be evident in the electron momentum density and the spin-resolved momentum density as revealed by Compton scattering. Further calculations of the electronic structure and magnetism by the KKR-CPA method in disordered Heusler-type ternary alloys have recently been published [14].

1.2. Compton scattering and electron momentum density

The Compton profile, $J(p_z)$, is the projection of the electron momentum density distribution along the scattering vector:

$$J(p_z) = \iint [n\uparrow(p) + n\downarrow(p)]\,\mathrm{d}p_x\,\mathrm{d}p_y \tag{1}$$

where $n\uparrow(p)$ and $n\downarrow(p)$ are majority and minority band components, respectively. The area under the Compton profile $J(p_z)$, integrated over all momenta, is equal to the total number of electrons taking part in Compton scattering: it is usually normalized to the number of electrons per formula unit if all the atomic binding energies can be neglected. The spin-resolved part, commonly called the magnetic Compton profile (MCP), can be isolated from the total Compton scattering in ferro- and ferrimagnets by using circularly polarized radiation, reversing the direction of the sample magnetization and subtracting the spin-up and spin-down signals. The quantity extracted is $J_{mag}(p_z)$ where

$$J_{mag}(p_z) = \iint [n\uparrow(p) - n\downarrow(p)]\,\mathrm{d}p_x\,\mathrm{d}p_y. \tag{2}$$

The magnetic Compton profile is normalized to the magnetic spin moment of the sample in Bohr magnetons, μ_B, per formula unit. The electron momentum, p_z, is expressed in atomic units (au) where $\hbar = m = e = 1$ and $c = 137$, then 1 au of momentum equals 1.99×10^{-24} kg m s^{-1}.

For isotropic electron distributions only, both $J(p_z)$ and $J_{mag}(p_z)$ are monotonically decreasing with increasing p_z as long as the integrands in equations (1) and (2) are positive.

This must be so for the total electron density distribution (equation (1)) but not necessarily so for the unpaired spin distribution (equation (2)). Thus a central 'dip' in a magnetic Compton profile of a single crystal either implies that $n\downarrow(p) > n\uparrow(p)$ at low momenta or that there is a significant degree of anisotropy in the electron magnetization. In order to differentiate between these two possibilities, it is necessary to consider data from several crystallographic directions, effectively reconstructing the three dimensional distribution $[n\uparrow(p) - n\downarrow(p)]$.

Combining the two types of Compton profile one can obtain the so-called majority and minority band Compton profiles:

$$\begin{aligned} J\uparrow(p_z) &= 1/2[J(p_z) + J_{mag}(p_z)] = \iint n\uparrow(p_z)\,\mathrm{d}p_x\,\mathrm{d}p_y \\ J\downarrow(p_z) &= 1/2[J(p_z) - J_{mag}(p_z)] = \iint n\downarrow(p_z)\,\mathrm{d}p_x\,\mathrm{d}p_y. \end{aligned} \tag{3}$$

These quantities include all the electrons in the filled inner shells which are spin paired and have a spherically symmetric density distribution. Thus the directional differences will relate only to the band electrons and it is these differences that are extracted from the data in order to compare with theory. Reviews of Compton scattering related to both charge and spin-dependent densities can be found in [15–17].

2. Objectives

2.1. Determination of the conduction electron polarization

Magnetic form factor measurements carried out by the polarized neutron diffraction technique [1, 2, 5, 8] indicate that the magnetic polarization of the conduction electrons in Fe_3Si is much smaller than in Fe_3Al, while the spatial characteristics of the 3d-like moment are quite similar. The earlier neutron data [1, 2] did not provide significant evidence for the presence of the negative conduction electron magnetization, despite its established presence in pure iron. For example Moss and Brown [1] concluded that, although regions of negative density are visible in Fe_3Si far from the atomic sites, its magnitude is at the limit of statistical significance. Pickart and Nathans [2], investigating Fe_3Al by the same technique, did not discuss conduction electron polarization at all. Dobrzyński *et al* [5] re-examined the published data sets for both alloys and concluded that the magnetization in the interstitial regions is rather low. Moreover, the maximum entropy analysis of the magnetization distribution on the basis of the diffraction data showed that the presence of negative magnetization in the interstitial regions in Fe_3Si is questionable and a magnetic Compton scattering study was suggested [8] since the incoherent scattering method is more sensitive to the delocalized electron density distribution.

2.2. Testing the predictions of band theory

These measurements provided an opportunity to test the KKR band structure calculations of Bansil *et al* [14] and Kaprzyk [18] by comparing them with accurate experimental data for both the charge and spin-dependent Compton profiles. The calculations were performed using the same scheme as already described in [19] for Cu_2MnAl, the Heusler alloy jointly studied earlier by the Warwick and Bialystok groups, in which the only carrier of the magnetic moment is manganese. The spin-density distributions in both position and momentum spaces are almost spherically symmetric in this alloy. The present study provides an opportunity to determine whether the KKR method can describe the charge density and its spin-dependent part as well as the directional anisotropies. The value of Compton data in understanding the contributions of the various electronic states to the magnetic moment in ferromagnetic Heusler alloys is

illustrated in a recent study [20] where the spin moments and spin-resolved Compton profiles have been modelled by the FLAPW method.

2.3. Understanding the difference in the properties of the two alloys

Although both materials have very similar structural parameters, Curie temperatures, saturation magnetization etc, the exchange stiffness constant and the mechanical properties of the two alloys are quite different [21]. Evidence for the origin of these differences should be embedded in the magnetic Compton profiles if they can be measured with sufficient accuracy.

By comparing magnetic Compton profiles of bcc Fe and DO3-type Fe_3Si and Fe_3Al, it should be possible to determine the dependence of the MCP on the local environment. Haydock and You [11] showed that the binding between aluminium and iron atoms is strong, quasi-covalent in character and essential for formation of the magnetic moment of iron at (A, C) sites. They also predicted that a similar situation should hold for the case of Fe_3Si but made no specific calculation. The analysis of the spin-density distributions [5, 8] indicates that it is easier to induce magnetic moment on iron substituting for aluminium than for silicon atoms. This shows that covalency-type effects should be different in both alloys. It is also known the band width of Fe_3Si is larger than that of Fe_3Al. In both cases the Fermi energy lies close to the strong peaks in the density of states curves. The shape of the latter is quite similar in both alloys. Nevertheless, the KKR calculations presented in section 3 show that the anisotropies in momentum space in these alloys are different. On the other hand, covalency implies a directional anisotropy in the electron momentum density over and above that due to the geometry of the Brillouin zone. Also the difference in lattice parameters implies that the mechanisms for cohesion may differ.

These objectives motivated us to measure accurate directional magnetic Compton profiles and study the anisotropies in the majority and minority bands. The three-dimensional reconstruction of spin-dependent electron momentum density in materials under study has been reported elsewhere [22].

3. Experimental procedure

The measurements were carried out at room temperature at the ESRF, Grenoble on beamline ID15 following the procedure described in detail elsewhere [23–25]. The samples were both parallelepipeds (Fe_3Al—10 mm × 10 mm × 0.5 mm and Fe_3Si—15 mm × 2 mm × 3 mm). The energy of the radiation delivered to the sample in a beam spot ∼1 mm (horizontal) ×2 mm (vertical) was 198.2 keV. The degree of circular polarization of the radiation (∼0.5) was achieved by viewing the source at 10–50 μrad above the orbital plane. The scattering angle was $\theta = 167.8^\circ$. The intrinsic germanium detector had an energy resolution equivalent to an electron momentum resolution (full width at half maximum) of 0.40 atomic units (au) at the Compton peak. A rotatable permanent magnet, which produced a field of 1 T, was used to reverse the magnetization in the sample every 30 seconds.

The directional magnetic Compton profiles of the thicker Fe_3Si were measured in reflection geometry. Transmission geometry was used for the thinner Fe_3Al sample but only two Compton profiles [100] and [111] could be measured. Since the alloys studied in this work are iron rich, a reference Compton profile from an iron single crystal was also measured. The measurement time was 20–25 hours for each crystallographic direction in the alloys. The total Compton profiles, $J(p_z)$, were extracted from the experimental spectra after background subtraction, standard energy dependent corrections (see [19, 25]) and the removal of multiple scattering by Monte Carlo simulation [26]. The multiple charge scattering amounted to about 10% and

15% of single scattering for Fe_3Al and Fe_3Si, respectively. Spin dependent multiple scattering, which is always much smaller (∼1%), was estimated to have no significant effect on either of the magnetic Compton profiles [24, 25, 27]. The total Compton profiles were normalized to 85.63 and 86.56 electrons under the profile in the momentum range from −10 to +10 au for Fe_3Al and Fe_3Si, respectively. The integrated counts under the Compton lines were approximately equal to 6×10^8, which resulted in a statistical accuracy of the total profile of 0.03% at $p_z = 0$ au and 0.15% at $p_z = 10$ au. The magnetic Compton profiles were formed from the difference of the data sets for $J\uparrow(p_z)$ and $J\downarrow(p_z)$ according to equation (2). Since both $J(p_z)$ and $J_{mag}(p_z)$ are symmetric about zero momentum the profiles were folded about $p_z = 0$ in order to improve their statistical accuracy.

4. Electronic structure calculations

The electronic band and momentum density computations of Fe_3Al and Fe_3Si are based on the KKR Green function method and use the muffin-tin approximation to the crystal potential [28–30]. All electrons were included, and the local spin-density approximation to the spin-polarized effective exchange–correlation potential was used, in the von Barth–Hedin [31] form. The band-structure problem was solved to a high degree of self-consistency (energy bands, Fermi energy and potentials converged to better than 1 meV) for the Fe_3Al and Fe_3Si fcc lattice (lattice constants equal to 10.93 and 10.69 au, respectively) using $l_{max} = 2$ for the maximum angular momentum cut-off. In order to calculate the Compton profiles the spin momentum densities $n(p)$ were calculated on a mesh containing $48 \times 196 \times 1837$ p points; where 48 denotes the multiplicity of the cubic point group, 196 the number of k points in the irreducible 1/48th of the Brillouin zone and 1837 the number of p points obtained from each k point by adding reciprocal lattice vectors (for details see [18]). The two-dimensional integrations involved in the evaluation of the Compton profile (equation (1)) were carried out by using the tetrahedral method of Lehmann and Taut [32]. This approach is very suitable for developing highly vectorized computer codes. The band electron Compton profiles along [100], [110] and [111] crystallographic directions were then determined up to $p_z = 10$ au, which corresponds to the maximum reciprocal lattice vector in the calculation. By making a variety of computations using different mesh sizes etc it was estimated that the calculated Compton profiles are reproducible to ∼5 parts in 10^4.

The magnetic moments calculated for perfectly ordered Fe_3Si and Fe_3Al are equal to 4.85 μ_B and 5.95 μ_B, respectively. This compares to measured values of 4.9 μ_B and 4.8 μ_B, respectively showing that the theoretical value for Fe_3Al is greatly overestimated. This is not simply a matter of scaling, the LSDA approach not only fails to reproduce the size of the spin moment in Fe_3Al but also its momentum distribution as revealed by $J_{mag}(p_z)$. This discrepancy between experimental and theoretical moments has been discussed elsewhere [14] and is similar to those found for other binary Fe–Al alloys [33]. Therefore, in order to obtain the correct total moment, it was necessary to fix the spin moments at both Fe sites and the moments quoted in [2] were chosen for this purpose, i.e. 1.5 μ_B at the A, C sites and 2.2 μ_B at the B site. Though not ideal, this represents the best current practical solution.

5. Results and discussion

The measured and calculated magnetic Compton profiles of Fe_3Si and Fe_3Al are shown in figure 1. The top panel shows the 100 magnetic Compton profiles predicted by the KKR method before and after convolution with the experimental resolution function; it is typical

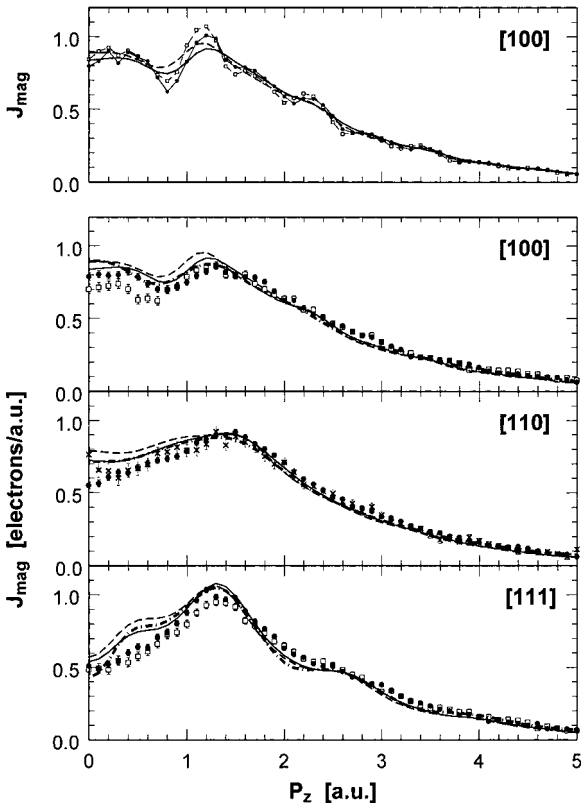

Figure 1. The magnetic Compton profiles of Fe_3Si and Fe_3Al. The upper diagram shows the KKR model profiles for the [100] direction (Fe_3Si—filled circles, Fe_3Al—open circles) before convolution with the experimental resolution function which is a Gaussian of FWHM 0.40 atomic units of momentum. The resolution smearing is apparent from the convoluted profiles (Fe_3Si—solid line, Fe_3Al—dashed line). Experimental data are shown in the lower three diagrams. The data points for Fe_3Si are denoted ● ● ● and those for Fe_3Al are denoted □ □ □. All theoretical profiles are convoluted with the resolution function. The solid line is the KKR profile for Fe_3Si and the dashed one for Fe_3Al. The theoretical FLAPW profiles of Kubo and Asano [34] calculated for the three main crystallographic directions in a pure iron single crystal are shown by the dot–dashed lines. For the [110] direction only, an experimental magnetic Compton profile of pure iron, measured under identical conditions to the alloys, is depicted × × ×. (The [110] direction was not measured in Fe_3Al.)

of the other directions in that there is not a wealth of fine structure hidden by the resolution smearing. Figure 1 also includes $J_{mag}(p_z)$ for pure iron as measured under identical conditions for the [110] direction, plus FLAPW calculated profiles [34] for all three directions. The first point to note is that experimental profiles of Fe and Fe_3Si are essentially identical, except very close to $p_z = 0$. Secondly the theoretical profiles for Fe [34] and Fe_3Si are very similar to each other at all electron momenta. Both observations indicate that the presence of silicon merely dilutes the total moment. In contrast the KKR calculation predicts systematic differences between Fe_3Si and Fe_3Al, but the only significant difference found experimentally between the two compounds is for the [100] direction and there the trend is opposite to that predicted, i.e. the Fe_3Al profile is lower, not higher, for $p_z < 1$ au. Above 4.0 au the profiles are very well fitted by the 3d-electron Fe free atom profile: this is expected since at high momenta deviations from the free atom prediction are physically unreasonable because they would imply

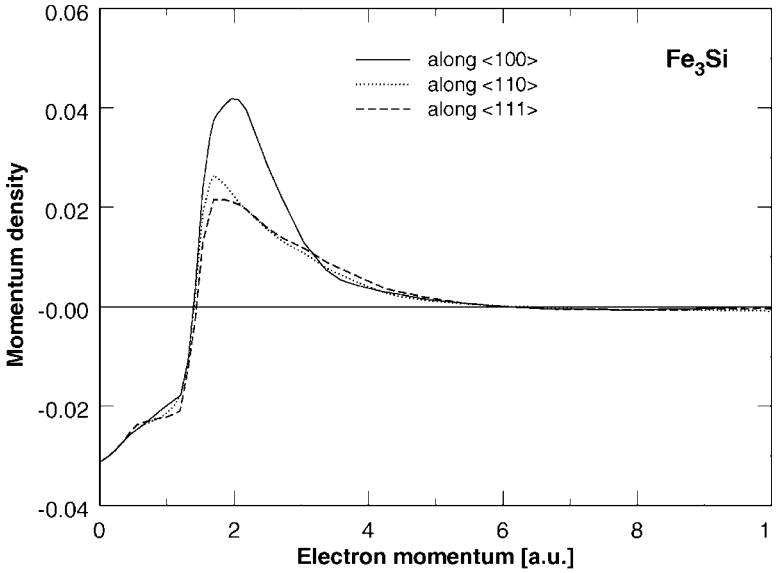

Figure 2. The spin resolved momentum density, $[n\uparrow(p) - n\downarrow(p)]$, along three directions in Fe_3Si reconstructed by the maximum entropy method from the measured magnetic Compton profiles. All directions show a negatively polarized spin density at momenta below ∼1.5 au. The ordinate is in units of electrons $(au)^{-3}$. Taken from [22].

large energy changes (the second moments of Compton profiles are directly related to the total electron energies).

5.1. Conduction electron polarization

Solid state effects are evident from the dips at low momenta in all the directional magnetic profiles. As explained in section 1.2 this suggests that there is a substantial delocalized conduction electron component in the minority band which has a negatively polarized magnetization. However since only two directions were measured for Fe_3Al it is difficult to rule out the origin of a central dip being simply due to the rapid decrease of the 3d momentum density near zero momentum, as was found in nickel [35].

For Fe_3Si, for which there are three sets of data, each showing a reduction in $J_{mag}(p_z)$ at low momenta, it is tempting to interpret the results as indicating a significant amount of reverse-polarized spin density, especially as the Si and Al atoms do not change the magnetic line shape significantly in comparison with iron. Recently two of the present authors [22] have published a maximum entropy reconstruction of the spin density in Fe, Cu_2MnAl and Fe_3Si, the last based on the data reported here. They found that, in contrast to the case of Cu_2MnAl, it was impossible to reconstruct physically reasonable distributions for Fe_3Si on the basis of a purely positive magnetization density distribution. That result for the spin-resolved momentum density along the three principal cubic directions is reproduced in figure 2 for the 'physically most reasonable' solution to the maximum entropy reconstruction. It shows that $n(p)$ is indeed negative below 1.5 au. The value of the negative spin moment is calculated by simple integration. It is just the negative area of the MEM-reconstructed three-dimensional spin density $[n\uparrow(p) - n\downarrow(p)]$ and is equal to 0.1–0.2 μ_B. Some caution is needed because the reconstruction is made with data from just three high symmetry directions but it can be proved that the assumption of a purely positive distribution leads to physically unacceptable

distributions. Figure 2 shows that a negative magnetization density ∼0.1–0.2 μ_B per Fe atom is necessary in Fe_3Si in order to fit the data, which is slightly higher than that found in pure iron based on the magnetic Compton scattering. This situation is in striking contrast to neutron diffraction results, which show relatively strong negative magnetization in Fe but very weak effects in both these alloys. On the other hand, the 3d-type spin-density distributions determined in neutron experiments correspond to the high momentum portions of MCPs which all are similar (i.e. 3d-like). It is well known that the diffraction experiments are susceptible to effects like extinction and multiple scattering. These, in turn, make it difficult to estimate accurately the conduction electron polarization, which is determined from the lowest order reflections. These problems with diffraction data have no counterpart in these incoherent Compton scattering studies. Thus we believe that the Compton scattering results give the more reliable picture and they indicate that Fe, Fe_3Si and, by analogy, Fe_3Al all exhibit similar levels of negative conduction electron polarization. Our observation of a negatively polarized spin density at low momenta is consistent with the observation of the spatially diffuse negative density reported in [1] and [5].

5.2. Testing the KKR band structure calculations

Figure 3 shows the experimental and theoretical anisotropy of the magnetic Compton profiles in Fe_3Si and Fe_3Al. The anisotropies are several times larger than those found in the related Heusler alloy Cu_2MnAl [19], which has been studied by both neutron diffraction and magnetic Compton scattering. This is consistent with the observation that in Fe_3Si and Fe_3Al there is an excess of spin-uncompensated electrons in e_g states [1, 2, 5–8]. Analysing the neutron data Dobrzyński [8] concluded that 'compared with the situation in bcc iron, the formation of DO_3 ordering with the presence of silicon increases the number of e_g states at the Fermi level, while the opposite is true for aluminium atoms'. The difference profiles [111] − [100] in the vicinity of 1–1.5 au, see figure 3, are consistent with this observation. Fortunately the resolution function full width at half maximum of 0.4 au in the magnetic Compton experiment does not smear out all the finer features of the Compton profile. Thus for example there is a shoulder at $p_z \approx 2.5$ au (see figure 1), which is due to *umklapp* of features present in the momentum density in the first Brillouin zone. This is also predicted in the band structure calculation and, with the exception of some discrepancies observed below 0.3 au, the anisotropy of the Compton profiles shows very good agreement between experiment and theory. In contrast to a transition metal such as Ni [35], but in line with earlier work on Fe, there does not appear to a wealth of fine structure in the MCP.

Figure 4 shows the experimental and theoretical directional difference Compton profiles for all the electrons, not just the spin resolved part. The figure clearly shows that the largest anisotropy [111] − [100] is very similar in both alloys, although they should be different according to the KKR model. Differences in the region of $p_z \sim 1.0$ au are visible in all the modelled anisotropies. A common feature of the anisotropies of Compton profiles of transition metals [36] is that experimental amplitudes are usually lower than those predicted theoretically out to momenta ∼3–5 au. This is usually ascribed to the failure of the local density approximation to provide an adequate description of electron correlation effects; however this is not the case here where differences are confined to the low momentum region. The KKR calculation seems adequate in this respect.

The majority and minority band profile anisotropies, formed from equations (3), are shown in figure 5. They reveal very different effects in the majority and minority bands. The smaller anisotropies in the majority band are of a similar size to those found in Cu_2MnAl [19] and this may be expected because the number of majority band electrons in similar. However a

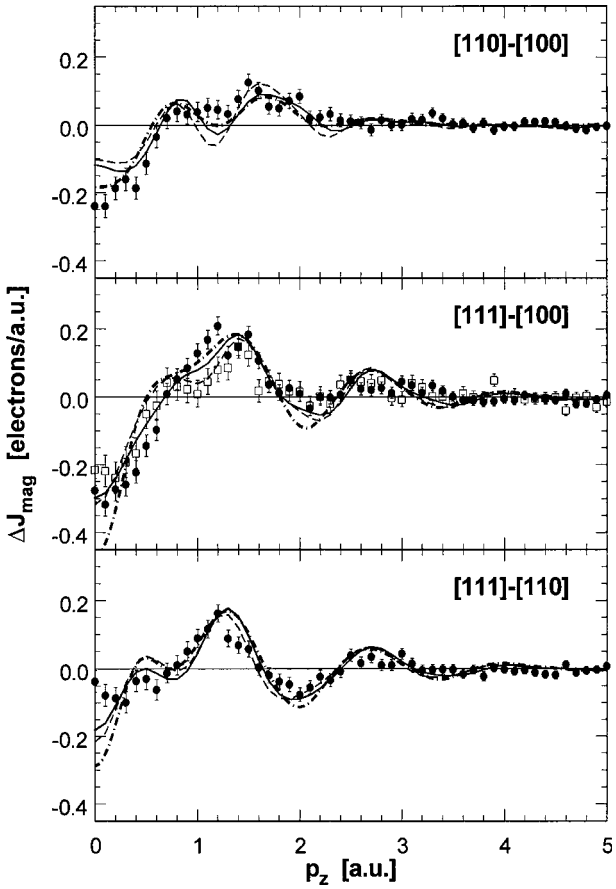

Figure 3. Difference profiles showing the anisotropies in the measured and calculated directional magnetic Compton profiles, $J_{mag}(p_z)$, of Fe_3Si and Fe_3Al. The symbols used are the same as in figure 1. Experimental data for Fe_3Al are shown for [111] − [100] only. For comparison the anisotropy in theoretical FLAPW profiles of Kubo and Asano [34] for pure iron is also shown. All the theoretical profiles are convoluted with a Gaussian of FWHM 0.40 au to mimic the experimental resolution.

huge anisotropy is evident at low momenta in the minority band of both Fe_3Si and Fe_3Al. This is not found in the Heusler alloy because in Cu_2MnAl the minority band gives practically no contribution to the magnetic moment, and hence to $J_{mag}(p_z)$. There the minority states originate principally from the almost-full 3d band due to the copper atoms, which do not show appreciable anisotropy. On the other hand in the alloys studied here, states in the lower half of the 3d minority band are occupied. These lower energy states correspond to more diffuse wavefunctions in position space and hence contribute strongly near $p_z = 0$.

These data provide the severest test of the ability of the KKR code to describe the aspherical part of the conduction electron density and it is clear that the degree of agreement is excellent, while at the same time, as figure 1 shows, the modelling of the total spin-resolved momentum density is poor at low momenta. However the failure of the method to predict the correct spin moment in Fe_3Al, and the subsequent need to assume fixed values for the moments, illustrates a serious shortcoming of the theory.

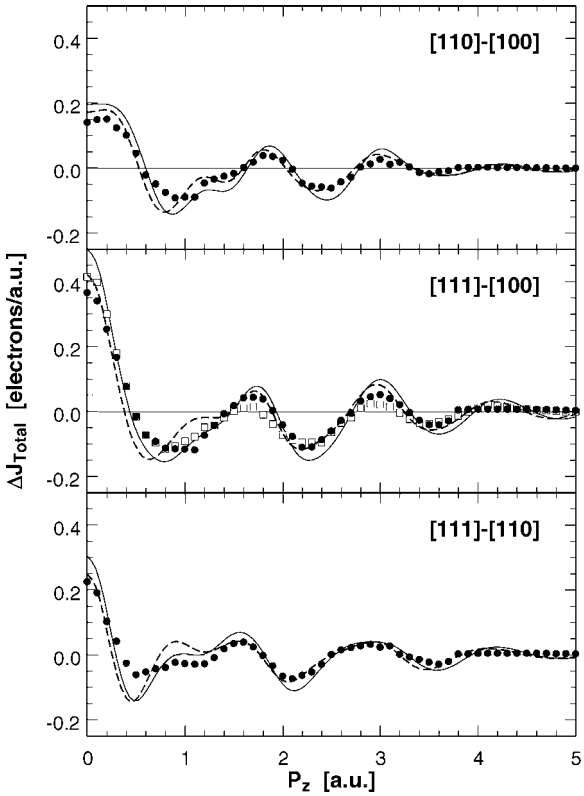

Figure 4. Difference profiles showing the anisotropies in the total electron (i.e. majority plus minority bands) directional Compton profiles, $J(p_z)$, for Fe_3Si and Fe_3Al. The statistical errors are smaller than the size of the points. All the theoretical profiles are convoluted with a Gaussian of FWHM 0.40 au to mimic the experimental resolution.

5.3. Understanding the differences in the properties of the two alloys

The scale of anisotropies in $J(p_z)$, and hence $n(p)$, is about half that found in pure iron [34]. Inspection of figure 4 shows that it is larger in $J_{[111]} - J_{[100]}$ and $J_{[111]} - J_{[110]}$ than $J_{[110]} - J_{[100]}$, which shows that the asphericity is associated with the [111] directional profile. The [111] direction is, of course, the nearest neighbour direction in both the bcc and DO_3 structures. The results presented in figure 4 follow the same trend as for the Heusler alloy Cu_2MnAl [19] but the amplitudes of the anisotropies measured here are between two and four times larger, which confirms the greater asphericity in the charge density of these alloys and, certainly for Fe_3Si, indicates a significant degree of covalency. As expected by Haydock and You [11], it does not seem that this effect is essentially different for Fe_3Al.

The somewhat larger anisotropy of the magnetic Compton profile of Fe_3Si with respect to Fe_3Al in the neighbourhood of $p_z = 1$ au is consistent with neutron results [3, 4–6], which show that the distribution in Fe_3Al is less aspherical, especially around A, C sites which have Si or Al atoms as nearest neighbours. Because the alloys are structurally isomorphic, one can ascribe the differences as due to a different type of bonding between the transition metal and Si or Al.

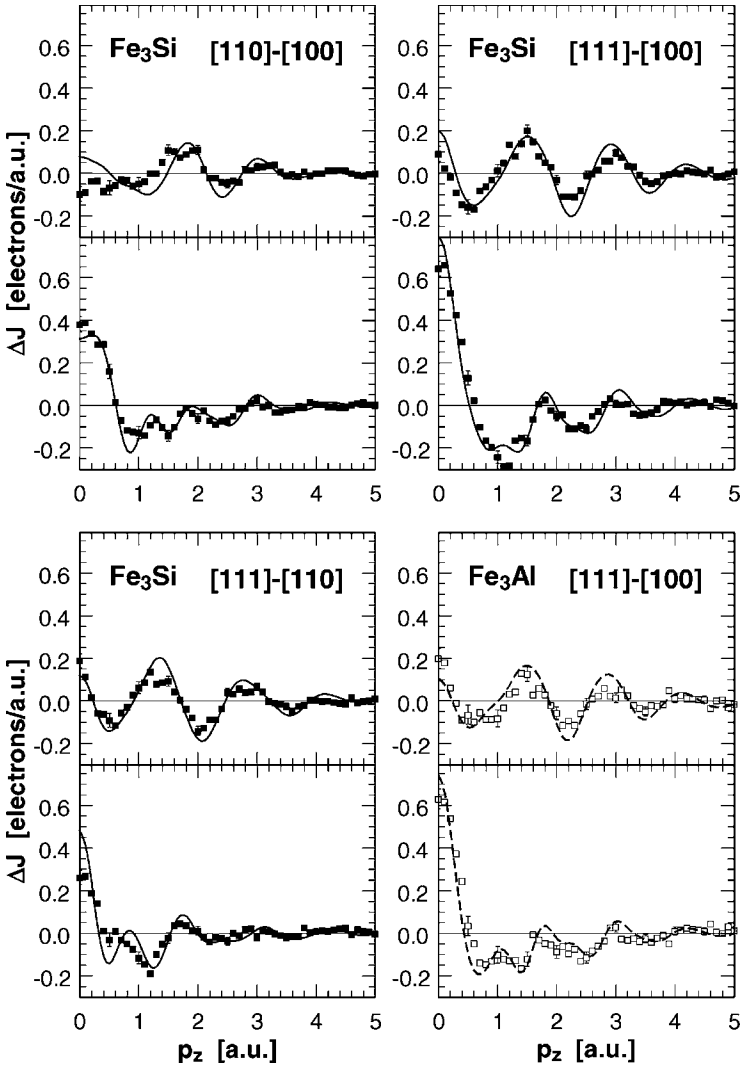

Figure 5. The anisotropies of majority (upper curve of each pair) and minority band (lower curve) Compton profiles of Fe_3Si and Fe_3Al, derived according to equation (3). The sum of top and bottom curves of each pair gives the anisotropy in the total Compton profiles (depicted in figure 4). Their differences are the anisotropies of the spin-dependent profiles (shown in figure 3). The KKR theory was convoluted with a Gaussian of FWHM 0.40 au to mimic the experimental resolution.

6. Summary

The experimental MCPs are similar for both materials but the agreement of the experiment with KKR calculations is better for Fe_3Si than for Fe_3Al at low momenta: the calculated spin moment in the low momentum region is generally overestimated, which is particularly significant for Fe_3Al. In this alloy our *ab initio* calculations encounter the same kind of difficulty as reported earlier for Fe–Al alloys [33] and transition metal ferromagnets [35]. Therefore it was necessary to fix the total spin moment, which results in considerable improvement in the description of the spin-dependent momentum density. However, within

the present limitations of KKR theory, it is still hard to say to what extent this disagreement in Fe_3Al can be due to disorder. Judging from the spin-density results [8], the presence of iron at D sites in Fe_3Al does not influence the magnetization in interstitial regions. Iron substituting for Al carries also magnetic moment similar to the one at the B site.

Large anisotropies are observed in the directional magnetic Compton profiles and in the derived majority and minority band profiles. In the case of Fe_3Si the KKR electronic structure calculation appears to be very good at describing these aspherical parts of the momentum density distribution.

The similarities between the Fe_3Si data and results for bcc iron, together with the maximum entropy reconstruction [22], indicate that there must be a conduction electron component that has negative spin polarization. In this respect magnetic Compton scattering is a better probe than diffraction techniques, which struggle to see the delocalized density distribution.

Acknowledgments

We are grateful to ESRF for providing beamtime for this investigation and to Professor P Suortti and Dr V Honkimäki of the ID15 beamline staff for their invaluable help. This study forms part of projects funded by the EPSRC in the UK and the Committee for Scientific Research in Poland (grant No 2P03B06108 and 2P03B01218). Professor Francesco Sacchetti is greatly thanked for providing the crystals and we are grateful to Dr K Perzyńska and Mrs M Biernacka for saturation magnetization measurements.

References

[1] Moss J and Brown P J 1972 *J. Phys. F: Met. Phys.* **2** 358
[2] Pickart S J and Nathans R 1961 *Phys. Rev.* **123** 1163
[3] *Landolt–Börnstein New Series* 1988 vol 19c (Berlin: Springer) pp 75–185
[4] Kato M, Nishino Y, Mizutani U and Asano S 2000 *J. Phys.: Condens. Matter* **12** 1769
[5] Dobrzyński L, Petrillo C and Sacchetti F 1990 *Phys. Rev.* B **42** 1142
[6] Brown P J, Ziebeck K R A and Huntley J M 1985 *J. Magn. Magn. Mater.* **50** 169
[7] Waliszewski J, Dobrzyński L, Malinowski A, Satuła D, Szymański K, Prandl W, Brückel Th and Schärpf O 1994 *J. Magn. Magn. Mater.* **132** 349
[8] Dobrzyński L 1995 *J. Phys.: Condens. Matter* **7** 1373
[9] Brauer S, Stephenson G B, Sutton M, Brüning R, Dufresne E, Mochrie S G J, Grübel G, Als-Nielsen J and Abernathy D L 1995 *Phys. Rev. Lett.* **74** 2010
[10] Garba E J D and Jacobs R L 1986 *J. Phys. F: Met. Phys.* **16** 1485
[11] Haydock R and You M V 1980 *Solid State Commun.* **33** 299
[12] Dobrzyński L, Blinowski K, Bednarski S, Kępa H, Giebułtowicz T and Minor W 1983 *Solid State Commun.* **46** 217
[13] Satuła D, Dobrzyński L, Waliszewski J, Szymański K, Rećko K, Malinowski A, Brückel Th, Schärpf O and Blinowski K 1997 *J. Magn. Magn. Mater.* **169** 240
[14] Bansil A, Kaprzyk S, Mijnarends P E and Tobola J 1999 *Phys. Rev.* B **60** 13 396
[15] Cooper M J 1985 *Rep. Prog. Phys.* **48** 415
[16] Sakai N 1996 *J. Appl. Crystallogr.* **29** 81
[17] Lovesey S W 1996 *J. Phys.: Condens. Matter* **8** L353
[18] Kaprzyk S 1997 *Acta Phys. Pol.* A **91** 135
[19] Żukowski E *et al* 1997 *J. Phys.: Condens. Matter* **9** 10 993
[20] Deb A and Sakurai Y 2000 *J. Phys.: Condens. Matter* **12** 2997
[21] Dobrzyński L, Giebułtowicz T, Kopcewicz M, Piotrowski M and Szymański K 1987 *Phys. Status Solidi* a **101** 567
[22] Dobrzyński L and Żukowski E 1999 *J. Phys.: Condens. Matter* **11** 8049
[23] McCarthy J E, Cooper M J, Lawson P K, Timms D N, Manninen S O, Hämäläinen K and Suortti P 1997 *J. Synchrotron Radiat.* **4** 102

[24] McCarthy J E, Cooper M J, Honkimäki V, Tschentscher T, Suortti P, Gardelis S, Hämäläinen K, Manninen S and Timms D N 1997 *Nucl. Instrum. Methods* A **401** 463
[25] Dixon M A G, Duffy J A, Gardelis S, McCarthy J E, Cooper M J, Dugdale S B, Jarlborg T and Timms D N 1998 *J. Phys.: Condens. Matter* **10** 2759
[26] Felsteiner J, Pattison P and Cooper M J 1974 *Phil. Mag.* **30** 537
[27] Sakai N 1987 *J. Phys. Soc. Japan* **56** 2477
[28] Bansil A 1987 *Electronic Band Structure and its Applications* vol 283, ed M Yussouff *Lecture Notes in Physics 283* (Heidelberg: Springer) p 273
Bansil A, Kaprzyk S and Tobola J 1992 *Applications of Multiple Scattering Theory to Materials Science (MRS Symp. Proc. 253)* ed W H Butler *et al* (Pittsburgh, PA: Materials Research Society) p 505
Bansil A, Rao R S, Mijnarends P E and Schwartz L 1981 *Phys. Rev.* B **23** 3608
[29] Kaprzyk S and Bansil A 1990 *Phys. Rev.* B **42** 7358
[30] Bansil A and Kaprzyk S 1991 *Phys. Rev.* B **43** 10 335
[31] Von Barth U and Hedin L 1972 *J. Phys. C: Solid State Phys.* **5** 1629
[32] Lehmann G and Taut M 1972 *Phys. Status Solidi* b **54** 469
[33] Moruzzi V L and Marcus P M 1993 *Phys. Rev.* B **47** 7878
[34] Kubo Y and Asano S 1990 *Phys. Rev.* B **42** 4431
[35] Dixon M A G, Duffy J A, Gardelis S, McCarthy J E, Cooper M J, Dugdale S B, Jarlborg T and Timms D N 1998 *J. Phys.: Condens. Matter* **10** 2759
[36] Cardwell D A and Cooper M J 1989 *J. Phys.: Condens. Matter* **1** 9357